J Solid State Electrochem (2007) 11:1139–1143
DOI 10.1007/s10008-006-0251-7

ORIGINAL PAPER

Synthesis and electrochemical properties of $LiNi_{0.9-x}Co_{0.1}Sn_xO_2$ as cathode materials for lithium secondary batteries

Xiaoling Ma · Chiwei Wang · Jinguo Cheng · Jutang Sun

Received: 22 September 2006 / Revised: 13 November 2006 / Accepted: 24 November 2006 / Published online: 20 December 2006

Abstract $LiNi_{0.9-x}Co_{0.1}Sn_xO_2$ (x=0.00, 0.02, and 0.03) were synthesized via the rheological phase reaction method and characterized by X-ray diffraction (XRD), scanning electron microscopy (SEM) and electrochemical tests. The sample of $LiNi_{0.9-x}Co_{0.1}Sn_xO_2$ (x=0.02) not only shows good cycle performance but also exhibits an excellent discharge capacity of 188 mAh/g in the first cycle at a current density of 100 mA/g in the voltage range of 3.0–4.3 V. The tin doping results in reducing the resistance and increasing conductivity of $LiNi_{0.9-x}Co_{0.1}Sn_xO_2$. This composite oxide is promising as cathode material for lithium-ion battery.

Keywords Cathode materials · Lithium-ion batteries · $LiNi_{0.9}Co_{0.1}O_2$ · Tin doping

Introduction

Lithium-ion batteries have been studied for the past several decades due to their high energy density and capacity. The cycle life and capacity of the lithium-ion cells critically depend on the structural and electrochemical properties of the cathode materials. Currently, the research on the cathode for lithium-ion batteries has been focused on three materials ($LiCoO_2$, $LiNiO_2$ and $LiMn_2O_4$) and their derivatives [1–6]. Generally, $LiCoO_2$ is used as commercial cathode materials due to its high reversibility, reasonable rate capacity and easy preparation, but it suffers from high cost and the relatively high toxicity of cobalt. $LiNiO_2$ is a more attractive material than $LiCoO_2$ because of its low cost and possibility of higher rechargeable capacity [7]. Nevertheless, stoichiometric $LiNiO_2$ is difficult to be obtained because of the loss of lithium from the host structure due to the high vapor pressure of lithium at high sintering temperature. Therefore, much research has been undertaken to search for new cathode materials to overcome these shortcomings.

In recent years, the lithium nickel cobalt mixed oxides have played an important role in the field of lithium-ion batteries [8, 9]. The solid solution, $LiNi_{1-y}Co_yO_2$ ($0<y<1$) is being closely scrutinized as a possible substitute for $LiCoO_2$ because it has both advantages of $LiNiO_2$ and $LiCoO_2$, which is based on the fact that $LiNiO_2$ and $LiCoO_2$ have the same layered α-$NaFeO_2$-type structure [10, 11]. Among them, $LiNi_{0.90}Co_{0.10}O_2$ appears to be much more promising. Elements such as Fe, Al, Mn, and Y have been used for partial substitution of Ni or Co to further enhance the electrochemical performance of the cathode materials [12–14]. The doped materials show better structural stability and cycling behavior than undoped ones.

In this study, for the first time, tin-doped $LiNi_{0.9}Co_{0.1}O_2$ cathode material is synthesized by the rheological phase reaction method, which does not need troublesome processes such as pelletizing, washing, stirring, and repeated heat treatment [15]. The effects of tin doping on the structure and electrochemical properties are discussed in detail.

Experimental

$LiNi_{0.9-x}Co_{0.1}Sn_xO_2$ (x=0.00, 0.02, and 0.03) were synthesized by the rheological phase reaction method [15]. $LiOH{\cdot}H_2O$, $Ni(OH)_2$, Co_2O_3, and SnO_2 were mixed fully in the stoichiometric molar ratio by grinding. Appropriate

X. Ma · C. Wang · J. Cheng · J. Sun (✉)
Department of Chemistry, Wuhan University,
Wuhan 430072, People's Republic of China
e-mail: jtsun@whu.edu.cn

amount of de-ionized water was added to get a rheological body and the mixture was heated at 80 °C for 5 h in a Teflon-lined stainless autoclave. After dried at 120 °C, the mixture was sintered at 730 °C for 10 h in oxygen atmosphere, and then cooled to room temperature to yield a black product.

The XRD patterns of $LiNi_{0.9-x}Co_{0.1}Sn_xO_2$ samples were obtained using a Shimadzu XRD-6000 diffractometer with a Cu $K\alpha_1$ radiation (λ=1.54056 Å). The morphological features and particle size were observed by a scanning electron microscope (Hitachi SEM X-650).

The charge/discharge tests were carried out using the coin-type test cell, which consisted of a $LiNi_{0.9-x}Co_{0.1}Sn_xO_2$ working electrode and a lithium foil electrode separated by a Celgard 2300 microporous membrane. Electrode was prepared by mixing $LiNi_{0.9-x}Co_{0.1}Sn_xO_2$ powders with 15% acetylene black and 5% PTEE binder, compressing the mixture onto an aluminum mesh current collector. A 1 mol/L solution of $LiPF_6$ dissolved in EC/DMC (1:1 volume ratio) is used as the electrolyte. The cells were assembled in an argon-filled glove box (Mikrouna, Super 1220/750, China). The cells were charged and discharged at a current density of 100 mA/g in the voltage range of 3.0–4.3 V. Electrochemical impedance were tested in the coin cells by using an EG&G basic electrochemical system (Princeton Applied Research, USA) in the frequency range of 100 kHz to 10 mHz with an excitation signal of 5 mV at room temperature. The working electrodes were discs of 10 mm diameter and about 5 mg of active material.

Results and discussion

The powder X-ray diffraction patterns of $LiNi_{0.9-x}Co_{0.1}Sn_xO_2$ (x=0.00, 0.02, and 0.03) are shown in Fig. 1. The sharp diffraction peaks indicate the synthesized materials possess high crystallinity. The crystal structure is identified as R-3 m space group and with a layered α-$NaFeO_2$-type structure. When the amount of tin dopant is small, the patterns exhibit two double peaks (006)-(102) and (108)-(110), which indicates that Li and Ni/Co are well ordered in a layered structure [16, 17]. When x>0.02, the small peaks of impurity Li_2SnO_3 are observed (JCPDS Card 04-0777). Although the dopant concentration is low, the structural properties of the host are still affected. The change of lattice parameters with x (tin dopant) are listed in Table 1. The lattice parameter along the c-axis increases from 14.1783 to 14.1796 Å and a slight change is observed in the a-axis with the tin dopant increases. The volume expansion of the unit cell assists the intercalation-deintercalation of Li ions during electrochemical processes.

The SEM images of $LiNi_{0.9}Co_{0.1}O_2$ and $LiNi_{0.88}Co_{0.1}Sn_{0.02}O_2$ powders are shown in Fig. 2. The grains

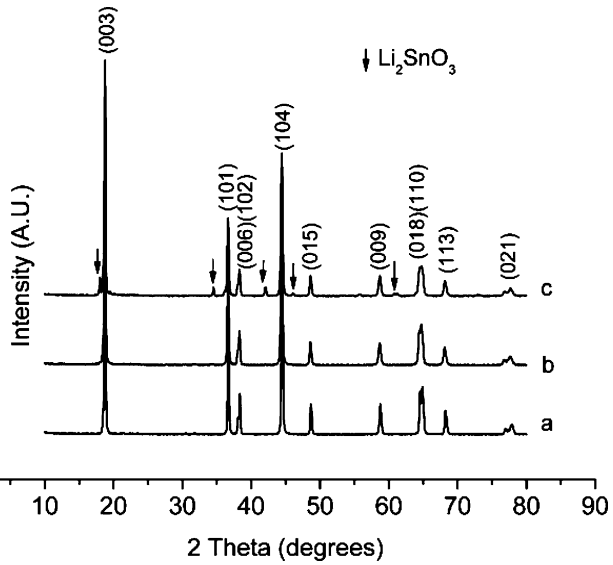

Fig. 1 Powder XRD patterns of $LiNi_{0.9}Co_{0.1}O_2$ (**a**), $LiNi_{0.88}Co_{0.1}Sn_{0.02}O_2$ (**b**) and $LiNi_{0.87}Co_{0.1}Sn_{0.03}O_2$ (**c**)

consist of fine crystal particles with the average size of 0.6 μm. The crystal particle size determines the effective surface area and smaller particles tend to improve the capacity of the battery by reducing the ion diffusion pathway during intercalation-deintercalation processes of Li ions [8]. At the same time, the tin-doped materials have similar size distribution and morphology compared with the $LiNi_{0.9}Co_{0.1}O_2$. This suggests that the tin is well permeated into the $LiNi_{0.9}Co_{0.1}O_2$.

The electrochemical properties of the materials were shown in Figs. 3, 4, 5, and 6. Figure 3 shows the initial charge-discharge curves of $LiNi_{0.9-x}Co_{0.1}Sn_xO_2$ (x=0.00, 0.02 and 0.03) electrodes. The results indicate that the initial discharge capacity of the bare $LiNi_{0.9}Co_{0.1}O_2$ cathode is 189 mAh/g, which is higher than that of the tin-doped $LiNi_{0.9-x}Co_{0.1}Sn_xO_2$ cathode. It is noted that tin is not electrochemically active when substituted at the Ni site. Thus, they are expected to decrease the capacity. However, the bare $LiNi_{0.9}Co_{0.1}O_2$ cathode loses its discharge capacity earlier than tin-doped materials. After 70 cycles, The $LiNi_{0.9}Co_{0.1}O_2$ cathode only has the capacity of 135 mAh/g, but the $LiNi_{0.88}Co_{0.1}Sn_{0.02}O_2$ cathode has the capacity of 150 mAh/g. Figure 4 indicates that tin plays a crucial role in improving the cycleability of $LiNi_{0.9}Co_{0.1}O_2$ cathode. Figure 5 shows the charge/discharge profiles and

Table 1 Lattice parameters of $LiNi_{0.9-x}Co_{0.1}Sn_xO_2$

x	a (Å)	c (Å)	V (Å^3)
0	2.8721(1)	14.1783(11)	101.29
0.02	2.8764(3)	14.1787(31)	101.60
0.03	2.8765(3)	14.1796(39)	101.61

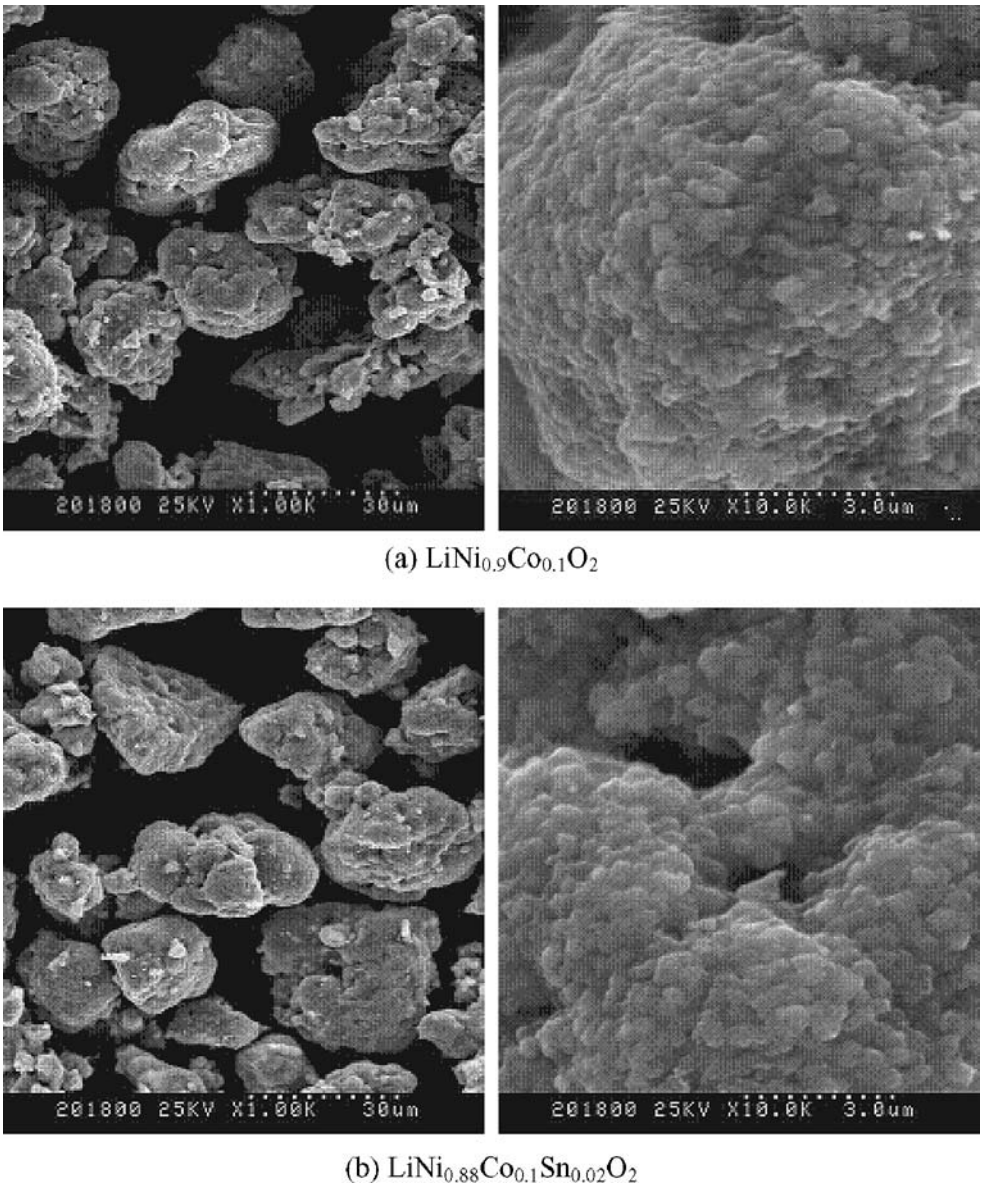

Fig. 2 SEM images of $LiNi_{0.9}Co_{0.1}O_2$ (**a**) and $LiNi_{0.88}Co_{0.1}Sn_{0.02}O_2$ (**b**) particles

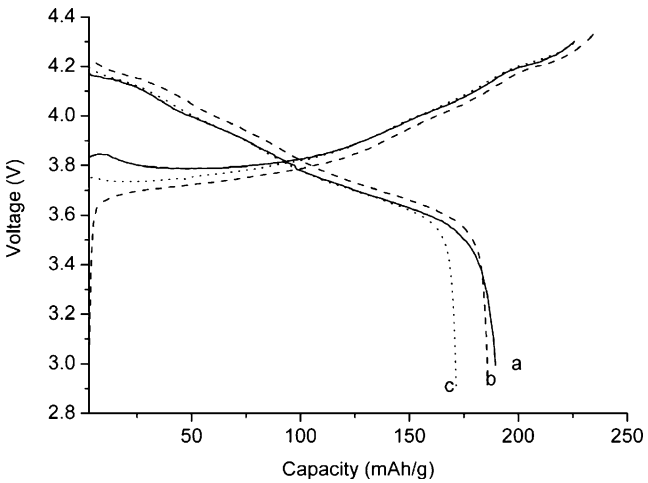

Fig. 3 Initial charge-discharge curves of $LiNi_{0.9-x}Co_{0.1}Sn_xO_2$ electrode at a current rate of 100 mA/g in 3.0–4.3 V (a, x=0; b, x=0.02; c, x=0.03)

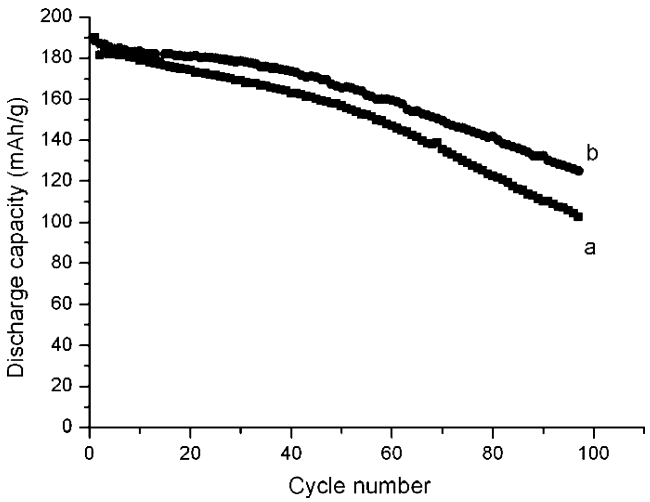

Fig. 4 Cycle performance of $LiNi_{0.9}Co_{0.1}O_2$ (**a**) and $LiNi_{0.88}Co_{0.1}Sn_{0.02}O_2$ (**b**) electrodes at a current rate of 100 mA/g in 3.0–4.3 V

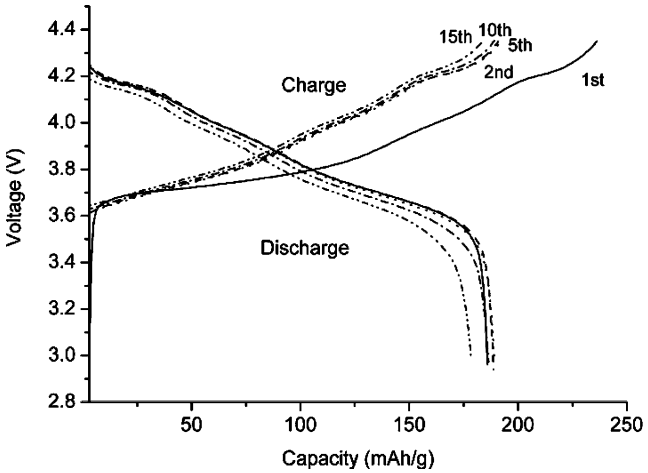

Fig. 5 The selected charge and discharge curves for $LiNi_{0.88}Co_{0.1}Sn_{0.02}O_2$ electrode at a current rate of 100 mA/g in 3.0–4.3 V

delivered capacity of $LiNi_{0.88}Co_{0.1}Sn_{0.02}O_2$ cathode for different cycles. From the Figs. 4 and 5, it can be concluded $LiNi_{0.88}Co_{0.1}Sn_{0.02}O_2$ cathode has good cycleability, and tin doping improves capacity fading. It suggests that the original layered crystal structure was maintained during intercalation and deintercalation of Li ions, which could be explained as the following: on the one hand, the increase of cell volume facilitates the intercalation and deintercalation of lithium [14]. On the other hand, the strength of Sn-O bonding is higher than Ni-O on the basis of standard Gibbs energy of the formation of the both oxides at 298 K [18]. So the crystal structure of $LiNi_{0.88}Co_{0.1}Sn_{0.02}O_2$ is more stabilized than that of $LiNi_{0.9}Co_{0.1}O_2$. Therefore, the tin-doped compound is a viable alternative for a better cathode material.

To provide more information for the improved electrochemical property, AC impedance measurements are performed at charge state (4.3 V) in the first cycle for the $LiNi_{0.9}Co_{0.1}O_2$ and $LiNi_{0.88}Co_{0.1}Sn_{0.02}O_2$ electrodes (Fig. 6). For the both electrodes, the impedance spectrum consists of a semicircular region at high-frequency range and a semicircular region at low-frequency range. The semicircle diameter of the $LiNi_{0.9}Co_{0.1}O_2$ electrode is three times larger than that of $LiNi_{0.88}Co_{0.1}Sn_{0.02}O_2$ electrode. The high frequency semicircle is attributed to the charge-transfer resistance of electrochemical reaction [19, 20]. This indicates that the charge-transfer resistance of tin-doped material is much lower than that of bare material. So it can be concluded that the material becomes more conductive with tin doping. Electrochemical impedance is a major part of internal resistance of a battery, the small impedance is favorable for the intercalation and deintercalation of lithium ions during the charge and discharge process. The results of the electrochemical impedances further confirm the improved electrochemical properties of tin-doped material.

Conclusions

The $LiNi_{0.9-x}Co_{0.1}Sn_xO_2$ (x=0.00, 0.02, and 0.03) cathode materials were synthesized by the rheological phase reaction method. The materials remain a layered α-$NaFeO_2$-type structure with the R-3 m space group. Electrochemical tests show that the tin-doped materials can effectively improve charge-discharge cycling performance, compared with the $LiNi_{0.9}Co_{0.1}O_2$. The improvement may be attributed to decreasing the electrochemical

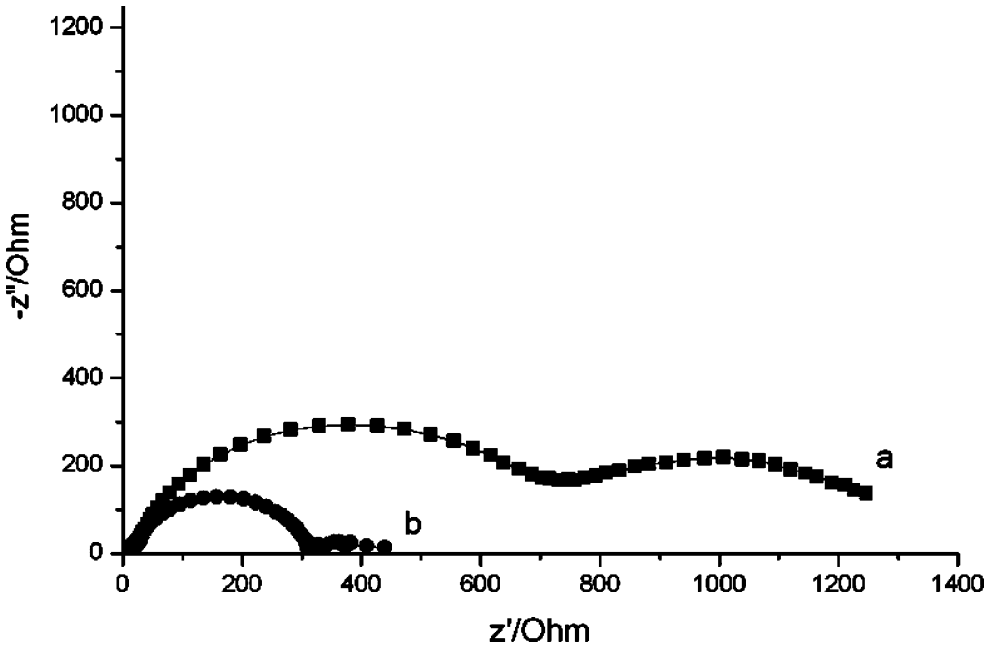

Fig. 6 Nyquist plots of $LiNi_{0.9}Co_{0.1}O_2$ (**a**) and $LiNi_{0.88}Co_{0.1}Sn_{0.02}O_2$ (**b**) electrodes at 4.3 V at room temperature. Frequency range, 10 mHz to 100 kHz

impedance and stabilization of the hexagonal $LiNi_{0.88}Co_{0.1}Sn_{0.02}O_2$, as confirmed by the AC impedance measurement and X-ray diffraction analysis.

Acknowledgement This work was supported by the National Natural Science Foundation of China (No. 20471044).

References

1. Zhong YD, Zhao XB, Cao GS (2005) Mater Sci Eng B 121:248
2. Shin H-S, Park S-H, Bae YC, Sun Y-K (2005) Solid State Ion 176:2577
3. Zhu XJ, Chen HH, Zhan H, Yang DL, Zhou YH (2004) Mater Chem Phys 88:145
4. Chen Y, Wang GX, Tian JP, Konstantinov K, Liu HK (2004) Electrochim Acta 50:435
5. Liu H, Wu YP, Rahm E, Holze R, Wu HQ (2004) J Solid State Eletrochem 8:450
6. Wu YP, Rahm E, Holze R (2002) Electrochim Acta 47:3491
7. Wang ZX, Liu LJ, Chen LQ, Huang XJ (2002) Solid State Ion 148:335
8. Cho J, Park B (2001) J Power Sources 92:35
9. Jin SJ, Song CH, Park KS, Stephan AM, Nahm KS, Lee YS, Kim JK, Chung HT (2006) J Power Sources 158:620
10. Tarascon M, Armand M (2001) Nature 414:359
11. Wu SH, Yang CW (2005) J Power Sources 146:270
12. Kim J, Kim BH, Baik YH, Chang PK, Park HS, Amine K (2006) J Power Sources 158:641
13. Croguennec L, Suard E, Willmann P, Delmas C (2002) Chem Mater 14:2149
14. Han CJ, Yoon JH, Cho WI, Jang H (2004) J Power Sources 136:132
15. Sun JT, Xie W, Yuan LJ, Zhang KL, Wang QY (1999) Mater Sci Eng B 64:157
16. Li W, Reimers JN, Dahn JR (1993) Solid State Ion 67:123
17. Peres JP, Delmas C, Rougier A, Broussely M, Perton F, Biensan P, Willmann P (1996) J Phys Chem Solids 57:1057
18. Lide DR (1995) Handbook of Chemistry and Physics, 76th edn. CRC Ress, London, pp 2
19. Suresh P, Shukla AK, Munichandraiah N (2002) J Appl Electrochem 32:267
20. Nobili F, Croce F, Scrosati B, Marassi R (2001) Chem Mater 13:1642